Catal Lett (2007) 119:257–264
DOI 10.1007/s10562-007-9226-2

# Effect of Ceria on the Storage and Regeneration Behavior of a Model Lean $NO_x$ Trap Catalyst

**Yaying Ji · Todd J. Toops · Mark Crocker**

Received: 6 June 2007 / Accepted: 17 July 2007 / Published online: 4 August 2007


**Abstract** In this study the effect of ceria addition on the performance of a model Ba-based lean $NO_x$ trap (LNT) catalyst was examined. The presence of ceria improved $NO_x$ storage capacity in the temperature range 200–400 °C under both continuous lean and lean-rich cycling conditions. Temperature-programmed experiments showed that $NO_x$ stored in the ceria-containing catalyst was thermally less stable and more reactive to reduction with both $H_2$ and CO as reductants, albeit at the expense of additional reductant consumed by reduction of the ceria. These findings demonstrate that the incorporation of ceria in LNTs not only improves $NO_x$ storage efficiency but also positively impacts LNT regeneration behavior.

**Keywords** $NO_x$ · Storage · Reduction · LNT · Ceria

## 1 Introduction

Lean-burn engines, including diesel and gasoline direct injection engines, are generally more fuel-efficient than stoichiometric gasoline engines and emit less carbon dioxide. Thus there are both economic and environmental incentives to increase the use of lean-burn vehicles. However, the development of effective after treatment methods for the abatement of lean exhaust emissions represents a challenge to the automotive industry. While conventional three-way catalysts are highly effective for control of nitrogen oxides ($NO_x$), CO and hydrocarbons (HCs) from stoichiometric exhaust, the technology for removal of $NO_x$ from lean exhaust is still not fully developed. Specifically, the excess oxygen present in lean exhaust competes with $NO_x$ for available reductants ($H_2$, CO, HCs), and significantly decreases $NO_x$ reduction efficiency.

Of the several technologies proposed for lean $NO_x$ removal, the lean $NO_x$ trap (LNT), also known as the $NO_x$ Storage-Reduction (NSR) catalyst or the $NO_x$ Adsorber Catalyst (NAC), is considered a promising candidate. LNT catalysts contain precious metals (generally Pt and Rh) and an alkali or alkaline-earth metal storage component (most commonly BaO) supported on a high surface area material (usually alumina). Under typical lean exhaust conditions, NO is oxidized to $NO_2$ over precious metal sites and reversibly stored as nitrates or nitrites on the storage materials. Stored $NO_x$ species are subsequently decomposed, released and reduced to $N_2$ during short periodic excursions to rich (i.e., net reducing) conditions. The trapping ability of the LNT catalyst is thus restored after a lean-rich cycle.

A major issue still remaining for LNT catalysts is that of deactivation due to sulfur poisoning. Decomposition of barium sulfate requires high temperatures (around 700 °C) and reducing conditions. Such treatments reduce the high fuel efficiency of lean-burn engines and result in catalyst deterioration due to sintering of the precious metal and $NO_x$ storage components, as well as the occurrence of unwanted reactions between washcoat components. Therefore, the improvement of LNT durability represents a key challenge.

Y. Ji · M. Crocker (✉)
Center for Applied Energy Research, University of Kentucky, 2540 Research Park Drive, Lexington, KY 40511-8479, USA
e-mail: crocker@caer.uky.edu

T. J. Toops
Fuels, Engines and Emissions Research Center, Oak Ridge National Laboratory, 2360 Cherahala Blvd, Knoxville, TN 37932-1563, USA

Ceria is an important component of LNTs formulated for lean burn gasoline applications, its role being to provide the necessary oxygen storage capacity when the engine is operating under stoichiometric conditions, i.e., when the LNT is required to function as a conventional three-way catalyst [1–3]. However, to date, the role of ceria in LNT catalysis has received little attention. Theis and co-workers reported that the addition of ceria improved $NO_x$ trap sulfur tolerance [4]. It is well known that ceria is able to store sulfur (as sulfate) [5], which may help to protect the main $NO_x$ storage component from sulfur poisoning. Additionally, Pt-promoted ceria is known to be a very effective catalyst for the water-gas shift (WGS) reaction [6, 7], and the hydrogen produced can be beneficial to LNT regeneration and desulfation. However, during rich purges oxygen stored by the ceria reacts with the reductants, increasing the total amount of reductant required for trap regeneration. In order to gain a better understanding of the benefits and disadvantages of ceria addition to LNT catalysts, we have studied the impact of ceria on NOx storage under both continuous lean flowing and lean-rich cycling conditions, as well as the impact on LNT regeneration characteristics.

## 2 Experimental

### 2.1 Catalyst Preparation

$Pt/CeO_2$ and $Pt/BaO/Al_2O_3$ powders were prepared by incipient wetness impregnation. $CeO_2$ (Rhodia, surface area of 119 $m^2/g$) was impregnated with an aqueous solution of tetraammineplatinum(II) nitrate. The impregnated sample was dried and then calcined in air at 500 °C for 3 h. $Pt/BaO/Al_2O_3$ was prepared in a sequential manner. $\gamma$-alumina (surface area of 132 $m^2/g$) was impregnated with aqueous $Ba(NO_3)_2$, dried and calcined at 500 °C in air. The Ba-loaded $Al_2O_3$ was subsequently impregnated with aqueous tetraammineplatinum(II) nitrate and further calcined at 500 °C. The Pt loading of both materials was 1 wt%, and the BaO content in the $Pt/BaO/Al_2O_3$ sample was 20 wt%. To prepare a ceria-containing LNT catalyst, a portion of $Pt/BaO/Al_2O_3$ was physically mixed with $Pt/CeO_2$ in a 74:26 weight ratio.

### 2.2 $NO_x$ Storage and Lean-rich Cycling Experiments

A microreactor loaded with ca. 150 mg of powder catalyst was employed to explore the $NO_x$ storage and regeneration behavior of the two model catalysts (see Fig. 1), the effluent gases being analyzed with a mass spectrometer (SRS RGA100). All flow conditions were operated at a gas hourly space velocity (GHSV) of 30,000 $h^{-1}$. Before each experiment the catalysts were pretreated in 1% $H_2$/Ar flow at 450 °C for 1 h. For $NO_x$ storage measurements, the catalyst was then subjected to typical rich conditions—3375 ppm $H_2$, 5625 ppm CO, 5% $CO_2$ and 5% $H_2O$ in Ar at 120 $cm^3$ (STP)/min (sccm) at 450 °C for an additional hour and then cooled to the desired temperature. $NO_x$ storage was recorded for 60 min while flowing typical lean conditions—300 ppm NO, 8% $O_2$, 5% $CO_2$ and 5% $H_2O$ in Ar at 120 sccm. This step was followed by a 15-min exposure to rich conditions, and then the 60-min cycle was repeated. This storage cycle was repeated until the measured storage value was consistent—up to six times.

$NO_x$ storage-regeneration experiments were performed while cycling between lean and rich conditions. Following pretreatment the catalyst was cooled to 400 °C, followed by cycling between lean and rich conditions until the catalyst reached a cycle-average steady-state. Once this steady state lean-rich cycle had been recorded, the catalyst was cooled to 300 °C while cycling. A steady-state cycle was then recorded at 300 °C followed by cooling to 200 °C. The total lean-rich cycle consisted of a 6 min lean phase, a 30 s transition to rich, a 30 s rich-phase, and then another 30 s transition to lean. A pneumatically-actuated 4-way valve was used to switch phases from lean to rich. For the purpose of $NO_x$ storage and release calculations, the $NO_x$ storage phase was taken to be 6.5 min in length (lean phase plus subsequent 30 s transition) and the regeneration phase was taken to be 1.0 min in length (rich phase plus subsequent 30 s transition). In part due to the length of these transitions, exotherms were minimal in the reactor system, the maximum observed being ca. 5 °C.

### 2.3 TPR and TPD Experiments

A temperature-programmed reduction (TPR) procedure was used to study how different reductants and $H_2O$ impact the LNT regeneration behavior. The catalysts were pretreated as before and then cooled in 1% $H_2$/Ar to 300 °C.

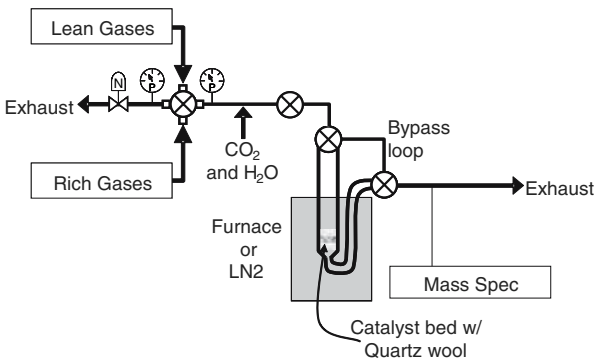


**Fig. 1** Schematic of microreactor and TPR system

$NO_x$ was stored at 300 °C in the absence of $CO_2$ and $H_2O$ for a period of typically 100–120 min in 300 ppm NO and 8% $O_2$ at 120 sccm. Under these conditions, the catalysts were still not saturated (typically ca. 0.4 mmol $NO_x$/g stored, versus >0.6 mmol $NO_x$/g stored at saturation). Subsequently, the catalysts were purged in Ar and cooled to 50 °C. For experiments in the absence of $H_2O$ the reductant flow was established in the exhausted portion of the 4-way valve while the reactor was being purged in Ar. At the beginning of the temperature ramp the flow was switched from the purge stream to the reductant stream. The furnace was ramped at 10 °C/min to 500 °C, and then held for 30 min. The microreactor system introduces water vapor after the 4-way valve, so a different approach was necessary when $H_2O$ was included in the TPR. Once the reactor had cooled to 50 °C, the reactor was sealed in Ar and the reductant stream was stabilized in the reactor bypass loop. At the beginning of the temperature ramp the flow was manually switched from the bypass loop to the reactor, and then the TPR proceeded as previously described.

## 3 Results and Discussion

### 3.1 $NO_x$ Storage Capacity

$NO_x$ storage measurements were performed on two catalyst samples, $Pt/BaO/Al_2O_3$ (hereafter denoted as PBA) and a physical mixture of $Pt/BaO/Al_2O_3$ and $Pt/CeO_2$ (74:26 weight ratio, denoted as PBAC), using feed gas containing 300 ppm NO, 8% $O_2$, 5% $CO_2$ and 5% $H_2O$. As shown in Fig. 2, $NO_x$ slip was observed from both catalysts immediately after exposure to the gas mixture, although $NO_x$ storage continued for more than 1 h before the catalysts were saturated. For both PBA and PBAC, maximum $NO_x$ storage after 1 h was observed at 300 °C. For PBA, the measured storage capacity at this temperature (0.27 mmol $NO_x$/g cat., see Table 1) corresponded to 84% utilization of the total Ba present. The lowest $NO_x$ storage on PBA was observed at 200 °C (0.19 mmol/g cat.), with only 59% of the loaded Ba being utilized. Compared to PBA, PBAC showed higher $NO_x$ storage capacity (0.28 mmol $NO_x$/g cat) at 300 °C after 1 h, indicating a slight benefit from the presence of ceria. At 200 °C, a significant improvement in $NO_x$ storage capacity was found for the ceria-containing catalyst, the quantity of stored $NO_x$ increasing from 0.19 mmol/g for PBA to 0.24 mmol/g for PBAC. Clearly, the addition of ceria significantly improved $NO_x$ storage at low temperature. However, at 400 °C, the presence of ceria resulted in decreased $NO_x$ storage capacity (0.17 mmol/g for PBAC versus 0.24 mmol/g for PBA). The $NO_x$ storage capacity of PBAC at this temperature corresponds to 71% of that for PBA, being almost equivalent to the percentage of the PBA component in catalyst PBAC. This implies that the $NO_x$ storage capacity of PBAC at high temperature derives from the Ba component only, with no benefit from the added ceria. In a previous DRIFTS study [8], we observed that cerium nitrates were formed on the surface of $Pt/CeO_2$ upon exposure to NO or $NO_2$. Upon heating in inert gas, these nitrates were largely stable to 300 °C, but completely disappeared upon heating to 400 °C. In a separate experiment under flowing $NO/O_2$, nitrate bands were observed at 400 °C, although with greatly reduced intensity relative to the spectrum obtained at 300 °C. Evidently the $NO_x$ storage capacity of ceria is greatly diminished at 400 °C, whereas at lower temperatures it can contribute significantly to the $NO_x$ storage capacity of LNT catalysts. The ability of ceria to store $NO_x$ was also reported by Haneda et al. [9], and it was found that doping Zr into $CeO_2$ can improve the $NO_x$ storage capacity.

The superior storage efficiency of PBAC relative to PBA is also manifested at short storage times. At 200 °C, a storage efficiency of 87% was obtained for PBAC for the first 6 min of the experiment, compared to only 69% for PBA (storage efficiency being defined as the percentage of $NO_x$ in the feed that is stored, see Table 1). Interestingly, the benefit of ceria addition to $NO_x$ storage efficiency during the first 6 min extended over the entire temperature range. After 60 min, the average storage efficiencies for PBAC and PBA were only 25% and 20%, respectively,

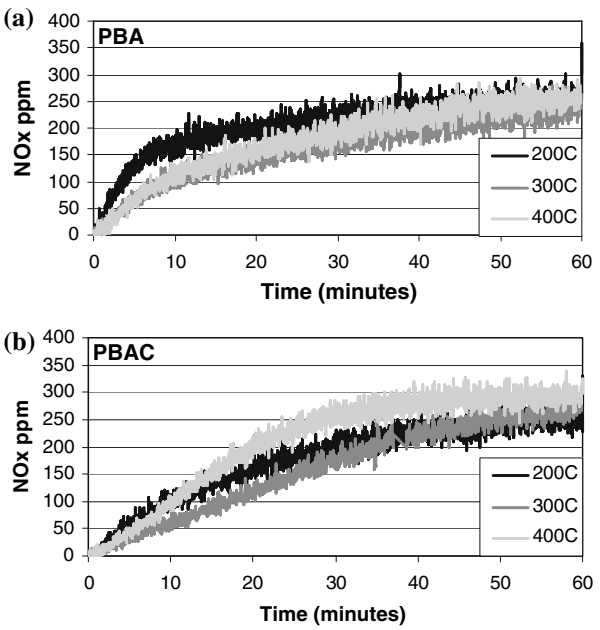


**Fig. 2** Outlet $NO_x$ concentration as a function of time during $NO_x$ storage under lean condition for (**a**) PBA and (**b**) PBAC. Gas composition: 300 ppm NO, 8% $O_2$, 5% $CO_2$, 5% $H_2O$, Ar balance, GHSV = 30,000 $h^{-1}$

**Table 1** Measured $NO_x$ storage capacity of PBA and PBAC at 6 min and 60 min under lean condition (300 ppm NO, 8% $O_2$, 5% $CO_2$, 5% $H_2O$, Ar balance, GHSV = 30,000 $h^{-1}$)

| Catalyst | Temp. (°C) | $NO_x$ storage at 6 min | | $NO_x$ storage at 60 min | |
|---|---|---|---|---|---|
| | | $NO_x$ stored (μmol/$g_{cat.}$) | Storage efficiency[a] (%) | $NO_x$ stored (μmol/$g_{cat.}$) | Storage efficiency[a] (%) |
| PBA | 200 | 36.4 | 69 | 190 | 20 |
| | 300 | 45.0 | 85 | 270 | 28 |
| | 400 | 44.8 | 85 | 240 | 25 |
| PBAC | 200 | 47.5 | 87 | 240 | 25 |
| | 300 | 49.7 | 93 | 280 | 29 |
| | 400 | 48.3 | 90 | 170 | 18 |

[a] Storage efficiency defined as: (moles $NO_x$ stored by catalyst)/(moles NO fed to reactor)

implying a significant decrease in $NO_x$ storage efficiency with time. Similar to the 60 min data, at short storage times the benefit in $NO_x$ storage capacity resulting from ceria addition decreases with increasing temperature.

### 3.2 $NO_x$ Storage-reduction Performance

To understand the effect of ceria addition on $NO_x$ storage during lean-rich cycling, $NO_x$ storage-reduction experiments were performed under long cycling conditions (6.0 min lean and 0.5 min rich with 30 s allowed for each transition). As shown in Fig. 3, after reaching a cycle-average steady state, slightly higher lean phase $NO_x$ slip was observed for PBA compared to PBAC at each of the three temperatures examined. Table 2 summarizes the $NO_x$ storage, unconverted $NO_x$ release (slip) and $NO_x$ reduction measured for the two catalysts during lean-rich cycling. Similar to the continuous lean flow experiments above, both catalysts showed optimal $NO_x$ storage at 300 °C with a measured $NO_x$ storage capacity of 47.4 μmol/g for PBA and 56.0 μmol/g for PBAC. However, the beneficial effect of ceria on $NO_x$ storage extended over the whole temperature range from 200 to 400 °C. Consistent with the improved $NO_x$ storage properties of PBAC at low temperature under continuous lean flowing conditions, the improvement in the lean phase $NO_x$ storage for PBAC relative to PBA was most evident at 200 °C during lean-rich cycling, while PBAC exhibited only a slight advantage at 400 °C. After switching to the rich phase, both catalysts showed very similar $NO_x$ release performance at the three temperatures, the largest $NO_x$ slip (1.6 μmol $NO_x$/g for PBA versus 1.7 μmol $NO_x$/g for PBAC) being observed at 200 °C and the smallest (0.5 μmol $NO_x$/g for both PBA and PBAC) at 300 °C. Based on the amount of $NO_x$ stored, only ~1% of the stored $NO_x$ was released without being reduced after switching to the rich phase at 300 °C. Given the low concentration of $NO_x$ slip during the rich phase, the $NO_x$ conversion averaged over lean-rich cycles was largely dependent on the effective lean phase $NO_x$ storage efficiency, from which it follows that catalyst PBAC afforded higher $NO_x$ conversion than PBA at each temperature.

It is also noteworthy that PBAC displayed a superior selectivity to $N_2$ over PBA for the entire temperature range (Table 2). A possible explanation for this observation lies in the fact that high $[H_2]$:$[NO_x]$ ratios favor $NO_x$ reduction to $NH_3$ [10]. Given the expected higher oxygen storage capacity of PBAC relative to PBA, the effective $[H_2]$:$[NO_x]$ ratio should be lower in PBAC due to partial consumption of the reductants by the reaction with stored oxygen. Additionally (or alternatively), for PBAC, ceria may play a role in helping to oxidize any $NH_3$ formed to $N_2$

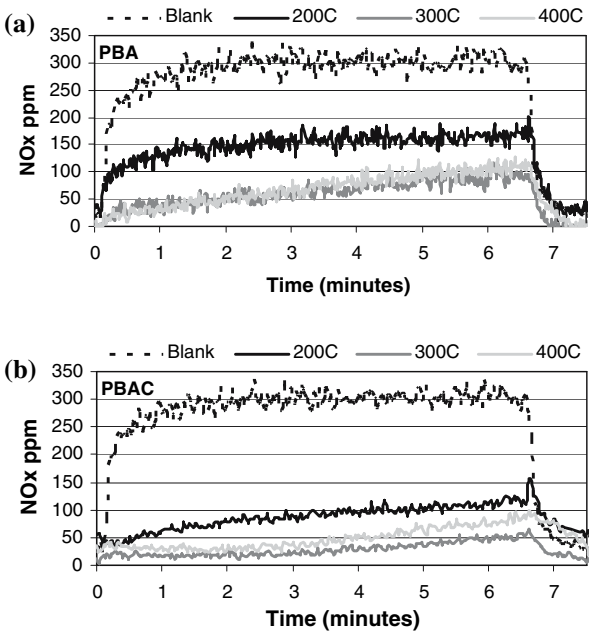


**Fig. 3** Outlet $NO_x$ concentration as a function of time during lean phase under lean-rich cycling over (**a**) PBA and (**b**) PBAC. Conditions are the same as in Table 2

**Table 2** Comparison of $NO_x$ storage, release and reduction from PBA and PBAC under steady-state cycling conditions[a]

| Catalyst | Temp. (°C) | $NO_x$ stored[b] (μmol/g) | $NO_x$ released[c] (μmol/g) | $NO_x$ converted (μmol/g) | $NO_x$ conversion[d] (%) | $N_2$ selectivity[e] (%) |
|---|---|---|---|---|---|---|
| PBA | 200 | 29.9 | 1.6 | 28.3 | 43.3 | 87 |
| | 300 | 47.4 | 0.5 | 46.9 | 75.9 | 69 |
| | 400 | 46.4 | 0.9 | 45.5 | 73.8 | 78 |
| PBAC | 200 | 42.8 | 1.7 | 41.0 | 66.6 | 92 |
| | 300 | 56.0 | 0.5 | 55.5 | 90.0 | 76 |
| | 400 | 51.8 | 1.1 | 50.7 | 82.1 | 88 |

[a] Lean-rich cycle: 300 ppm NO, 8% $O_2$, 5% $CO_2$, 5% $H_2O$ in Ar (6 min); 3375 ppm $H_2$, 5625 ppm CO, 5% $CO_2$, 5% $H_2O$ in Ar (0.5 min); GHSV = 30,000 $h^{-1}$

[b] The amount of $NO_x$ stored during the lean phase

[c] The amount of unconverted $NO_x$ released during the rich purge

[d] Total $NO_x$ conversion = (($NO_x$ stored during lean phase—$NO_x$ released during rich purge)/total inlet NO during the entire cycle) × 100%

[e] $N_2$ selectivity = (moles $NO_x$ converted to $N_2$)/(total $NO_x$ converted) × 100%

as the reaction front propagates along the length of the catalyst bed, as suggested by the results of recently published spatially resolved mass spectrometric studies [11].

It must be appreciated that under cycling conditions the lean phase $NO_x$ storage efficiency represents the product of the intrinsic storage efficiency (i.e., as measured under lean-only conditions) and the rich phase regeneration efficiency. Thus the superior performance of PBAC under cycling conditions can be a function of the intrinsic storage efficiency and/or the rich phase regeneration efficiency. To further understand the difference in regeneration behavior between PBAC and PBA, the thermal stability and reactivity of $NO_x$ stored on both PBAC and PBA was studied under different atmospheres (inert and reducing) by means of temperature-programmed techniques.

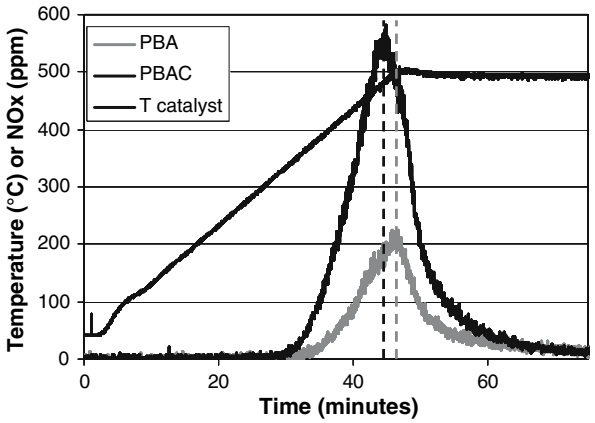


**Fig. 4** $NO_x$ evolved during Ar-TPD of PBA and PBAC

### 3.3 Thermal Stability of Stored $NO_x$

The thermal stability of $NO_x$ stored on the two catalysts was explored by means of temperature-programmed desorption (TPD) in flowing Ar. $NO_x$ was first stored on the catalysts at 300 °C for ca. 2 h using a feed containing 300 ppm NO and 8% $O_2$. The samples were then cooled to room temperature in flowing Ar, prior to ramping to 500 °C at a rate of 10 °C/min. As shown in Fig. 4, $NO_x$ evolution was not detected below 300 °C. This is in line with literature reports that thermal desorption of $NO_x$ does not occur below the temperature at which adsorption was performed [12–14]. Decomposition of the adsorbed $NO_x$ species commenced slightly above 300 °C, as evidenced by the evolution of $NO_x$, this process extending up to 500 °C for both catalysts. However, the temperature corresponding to maximum $NO_x$ release was different for the two catalysts. PBAC showed a maximum $NO_x$ release at ~470 °C, whereas PBA demonstrated a maximum at ~500 °C. During the TPD, 85% of $NO_x$ stored on PBAC was released, compared to 46% for PBA. From this it follows that a significant fraction of the adsorbed $NO_x$ species in PBAC exhibited lower thermal stability than those present in PBA, a finding that can be attributed to the lower thermal stability of cerium nitrates formed in PBAC in comparison with barium nitrate species.

### 3.4 Reduction Reactivity of Stored $NO_x$

The reactivity of stored $NO_x$ was investigated by means of temperature-programmed reduction (TPR) experiments. After $NO_x$ storage at 300 °C, the catalysts were cooled to ~50 °C in flowing Ar; TPR followed with either 2000 ppm $H_2$ ($H_2$-TPR), 3000 ppm CO (CO-TPR), or 3000 ppm CO + 5% $H_2O$ (CO + $H_2O$-TPR). In the case of $H_2$-TPR, minimal $NO_x$ release was observed from either sample, indicating that almost all of the stored $NO_x$ was

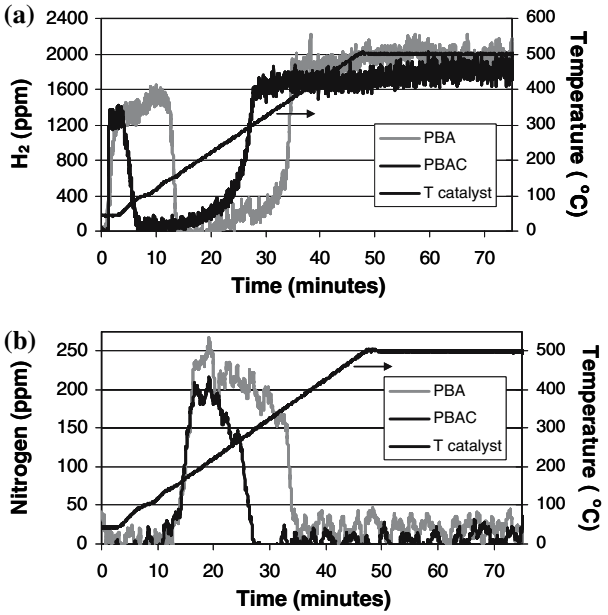


**Fig. 5** Gas concentrations in effluent during $H_2$-TPR of $NO_x$ stored on PBA and PBAC:(**a**) $H_2$ and (**b**) $N_2$

reduced to $N_2$, $NH_3$ and/or $N_2O$ (accurate quantification of the latter two species being impossible with the analytical system used). Figure 5 shows the concentrations of $N_2$ and $H_2$ in the effluent as a function of time/temperature during $H_2$-TPR. Compared to Ar-TPD, the catalysts were regenerated at significantly lower temperatures. On PBA, both $H_2$ consumption and $N_2$ production began simultaneously at 150 °C and ceased at ca. 385 °C; however, for PBAC, $H_2$ consumption started 70 °C lower than $N_2$ production, 80 °C versus 150 °C (Table 3). This low temperature consumption is associated with reduction of the ceria from an oxidized to a reduced state. $N_2$ production and $H_2$ consumption simultaneously ceased at 295 °C for PBAC, i.e., 90 °C lower than PBA. These findings suggest that the $NO_x$ species in PBAC are more easily decomposed in the presence of $H_2$ than are those in PBA.

CO-TPR demonstrated a small increase in the level of unconverted $NO_x$ release, respectively 6 and 19 μmol $NO_x$/$g_{cat}$ for PBA and PBAC (versus 543 and 596 μmol $NO_x$/$g_{cat}$ stored, respectively). For PBA, $NO_x$ evolution occurred in the range 139 to 290 °C, as compared to the range 114 to 195 °C for PBAC (not shown). The onset of $N_2$ production from the reduction of stored $NO_x$ by CO occurred at 195 °C for both catalysts, which is a significantly higher temperature than the 150 °C observed during $H_2$-TPR (Fig. 6a). $N_2$ production terminated at 427 °C on PBAC, while it extended up to 497 °C on PBA. Upon heating to 500 °C, 30% of the $NO_x$ stored on PBAC was reduced to $N_2$ by CO, compared to 42% for PBA. This suggests that there may be some nitrate remaining on the catalysts even after heating to 500 °C. It is apparent that CO shows lower reduction efficiency than $H_2$, as reported by several research groups [15–17]. In TPR with CO, the $NO_x$ released from the surface can be replaced by a crust of

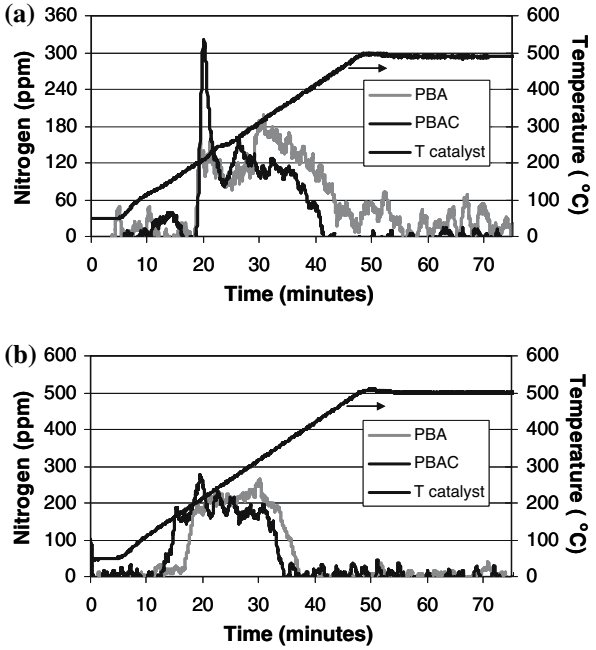


**Fig. 6** $N_2$ evolved during TPR of $NO_x$ stored on PBA and PBAC for (**a**) CO-TPR and (**b**) CO + $H_2O$-TPR

**Table 3** Comparison between PBA and PBAC of $N_2$ release and $H_2$ consumption during TPR of stored $NO_x$

| Condition[a] | Catalyst | $NO_x$ stored before TPR (μmol/$g_{cat}$) | $NO_x$ conv. to $N_2$ (%) | $N_2$release (°C) | | $H_2$ consumption (°C) | |
|---|---|---|---|---|---|---|---|
| | | | | Start | End | Start | End |
| $H_2$-TPR | PBA | 476 | 54 | 150 | 385 | 150 | 385 |
| | PBAC | 408 | 34 | 150 | 295 | 80 | 295 |
| CO-TPR | PBA | 543 | 42 | 195 | 497 | – | – |
| | PBAC | 596 | 30 | 195 | 427 | – | – |
| CO + $H_2O$-TPR | PBA | 339 | 72 | 180 | 391 | – | – |
| | PBAC | 388 | 62 | 135 | 362 | – | – |

[a]Gas compositions for TPR: 2,000 ppm $H_2$ in Ar ($H_2$-TPR), 3,000 ppm CO in Ar (CO-TPR), and 3,000 ppm + 5% $H_2O$ in Ar (CO + $H_2O$-TPR)

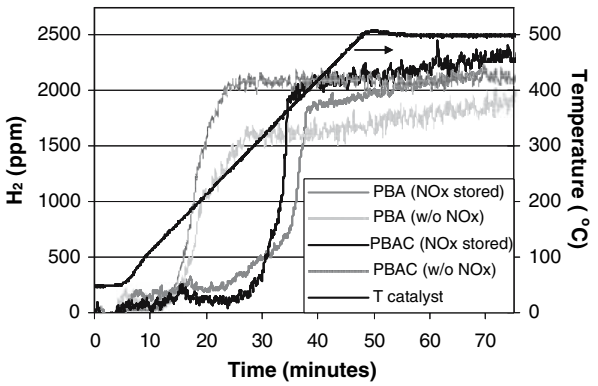


**Fig. 7** $H_2$ produced during CO + $H_2O$-TPR from both $NO_x$-loaded and $NO_x$-free catalysts

$BaCO_3$ which impedes migration of the remaining subsurface $NO_x$. We have performed a similar study using DRIFT spectroscopy that also suggests CO-only reduction results in unremoved nitrates (Unpublished results).

CO-TPR of stored $NO_x$ was also studied in the presence of $H_2O$ (CO + $H_2O$-TPR). As shown in Fig. 6b, the addition of $H_2O$ significantly altered the reduction behavior of $NO_x$ with CO. Compared to CO-TPR, the onset of $N_2$ production was shifted to lower temperature—corresponding to 135 °C for PBAC and 180 °C for PBA. Furthermore, on PBAC the detection of $N_2$ ceased at a lower temperature relative to CO-TPR—362 °C versus 427 °C. As shown in Fig. 7, $H_2$ was evolved over both catalysts during CO + $H_2O$-TPR, in each case attaining a maximum concentration circa 400 °C. In order to better understand this process, CO + $H_2O$-TPR was performed using catalysts which had not been exposed to $NO_x$. The resulting data show that both catalysts are highly active for the water-gas shift reaction. $H_2$ production commenced at temperatures as low as 140 °C, with PBAC exhibiting slightly higher activity than PBA across the entire temperature range. This most likely accounts for the more facile reduction of the stored $NO_x$ in PBAC during CO + $H_2O$-TPR.

Both $H_2$-TPR and CO-TPR results suggest that the adsorbed $NO_x$ species in PBAC are more easily decomposed in the presence of reducing agents than those in PBA. We hypothesize that the improved regeneration characteristics of PBAC are likely a consequence of the competitive capture of $NO_x$ by the $Pt/CeO_2$ component, which results in reduced formation of bulk $Ba(NO_3)_2$ in PBAC relative to PBA. This is akin to the idea that the ability of ceria to store sulfur (as sulfate) can be expected to help protect the main LNT $NO_x$ storage component from sulfur poisoning [4]. It is well known that upon exposure to $NO_x$, surface nitrates are initially formed on BaO, while increased exposure results in the subsequent formation of bulk nitrates. Furthermore, Peden et al. [17] have previously shown that bulk $Ba(NO_3)_2$ is significantly more difficult to reduce than surface $Ba(NO_3)_2$. Studies are currently in progress to address this issue.

## 4 Conclusions

These findings show that the addition of ceria to Ba-based LNT catalysts is beneficial with respect to $NO_x$ storage capacity at temperatures up to 400 °C, as demonstrated by the results of both lean flowing experiments (in which the intrinsic $NO_x$ storage capacity is measured), and lean-rich cycling experiments (in which the *effective* storage capacity is determined, given that intrinsic $NO_x$ storage capacity may not be completely regenerated). Rich phase $NO_x$ slip during cycling was found to be similar for both catalysts studied, with the consequence that overall $NO_x$ conversion was significantly higher for the ceria-containing catalyst. The ceria-containing catalyst also exhibited superior regeneration characteristics. $H_2$- and CO-TPR experiments suggest that adsorbed $NO_x$ species are more easily decomposed in the presence of reducing agents than are those in the ceria-free analog. This is likely a consequence of the competitive capture of $NO_x$ by the $Pt/CeO_2$ component, which results in reduced formation of (less reactive) bulk $Ba(NO_3)_2$. It can be inferred that under some rich operating conditions in the temperature range used in this study (200–500 °C) a portion of the bulk nitrate is not decomposed and thus cannot participate in $NO_x$ abatement through storage and regeneration. Instead, surface nitrates play the major role in $NO_x$ storage and reduction during lean-rich cycling.

**Acknowledgments** This publication was prepared with the support of the U.S. Department of Energy, under Award No. DE-FC26–05NT42631. However, any opinions, findings, conclusions, or recommendations expressed herein are those of the authors and do not necessarily reflect the views of the DOE.

## References

1. Matsumoto S (1994) Toyota Tec Rev 44:10
2. Yao HC, Yao YF (1984) J Catal 86:254
3. Fornasiero P, Balducci G, Di Monte R, Kaspar J, Sergo V, Gubitosa G, Ferrero A, Graziani MJ (1996) J Catal 164:173
4. Theis J, Ura J, Goralski C Jr, Jen H, Thanasiu E, Graves Y, Takami A, Yamada H, Miyoshi S (2003) SAE Technical Paper Series 2003-01-1160
5. Truex T (1999) SAE Technical Paper Series 1999-01-1543
6. Jacobs G, Williams L, Graham U, Sparks DE, Davis BH (2003) Appl Catal A 252:107
7. Phatak AA, Koryabkina N, Rai S, Ratts JL, Ruettinger W, Farrauto RJ, Blau GE, Delgass WN, Ribeiro FH (2007) Catal Today 123:224
8. Ji Y, Toops TJ, Uschi G, Jacobs G, Crocker M (2006) Catal Lett 110:29

9. Haneda M, Morita T, Nagao Y, Kintaichi Y, Hamada H (2001) Phys Chem Chem Phys 3:4696
10. Pihl JA, Parks JE, Daw CS, Root TW (2006) SAE Technical Paper Series 2006-01-3441
11. Parks J, Huff S, Swartz M, West B (2007) presentation at 10th CLEERS Workshop, Dearborn, MI
12. Nova I, Lietti L, Castoldi L, Tronconi E, Forzatti P (2006) J Catal 239:244
13. Szanyi J, Kwak JH, Hanson J, Wang C, Szailer T, Peden CHF (2005) J Phys Chem B 109:7339
14. Piacentini M, Maciejewski M, Burgi T, Baiker A (2004) Top Catal 30/31:71
15. Joza P, Jobson E, Larsson M (2004) Top Catal 30/31:177
16. Poulston S, Rajaram R (2003) Catal Today 81:603
17. Szailer T, Kwak JH, Kim DH, Hanson JC, Peden CHF, Szanyi J (2006) J. Catal. 239:51